Biochimica et Biophysica Acta, 1144 (1993) 149–160
© 1993 Elsevier Science Publishers B.V. All rights reserved 0005-2728/93/$06.00

BBABIO 43866

Slow ('resting') forms of mitochondrial cytochrome *c* oxidase consist of two kinetically distinct conformations of the binuclear Cu_B/a_3 centre – relevance to the mechanism of proton translocation

Chris E. Cooper [a], Susanne Jünemann [b], Nikolaos Ioannidis [b] and John M. Wrigglesworth [b]

[a] *Department of Paediatrics, University College London School of Medicine, The Rayne Institute, London (UK) and* [b] *Metals in Biology and Medicine Centre, Division of Life Sciences, King's College London, London (UK)*

(Received 5 March 1993)

Key words: Cytochrome *c* oxidase; Copper center; Proton translocation; Enzyme conformation; (Mitochondria)

We have purified slow ('resting') cytochrome oxidase from bovine heart, free of contamination with fast ('pulsed') enzyme. This form of the enzyme shows two kinetic phases of reduction of haem a_3 by dithionite ($k = 0.020 \pm 0.005$ s^{-1} and $k = 0.005 \pm 0.002$ s^{-1}). The presence of ligands that bind to the oxidized or reduced binuclear centre (formate or carbon monoxide respectively) has no effect on these rates. Varying the dithionite concentration also has no effect on either phase, although at low dithionite concentrations a lag phase is observed as the rate of haem *a* reduction is slower. The results are consistent with a model for reduction of the slow enzyme where the rate of electron transfer to the binuclear centre is the limiting step, rather than an equilibrium model where the haem a_3 redox potential is low. Increasing the pH decreases the rate of the slower phase of dithionite reduction, but has no effect on the faster phase. EPR studies show that the slow phase (only) correlates with the disappearance of the $g' = 12/g' = 2.95$ signals, with the same pH dependence; again the presence of formate has no effect on these results. Deconvolution of the oxidized optical spectra shows that the enzyme reduced in the slow phase has a blue-shifted Soret band, relative to that reduced in the faster phase. Incubation of the oxidized enzyme at high pH causes a line-broadening of both the $g' = 12$ and $g' = 2.95$ EPR signals with no obvious effect on the amount of signal. The results are interpreted in a model where the presence of a carboxylate bridge between haem a_3 and Cu_B defines the slow enzyme. It is suggested that the two rates of dithionite reduction are the result of different ligation to Cu_B – where water is the ligand the binuclear centre is Fe^{IV}/Cu^{I} (EPR-silent) and where hydroxide is the ligand the binuclear centre is Fe^{III}/Cu^{II} ($g' = 12/g' = 2.95$ EPR signals).

Introduction

Cytochrome *c* oxidase converts the redox energy from the oxidation of ferrocytochrome *c* and the reduction of molecular oxygen into a proton electrochemical gradient across the inner mitochondrial membrane [1]. There are three separate processes associated with proton motive force generation. The first is the movement of an electron from the cytochrome *c* binding site (external) to the oxygen reduction site (probably in the middle of the membrane) [2]. The second is the uptake of protons to this same site from the mitochondrial matrix [3]. The first two processes therefore are both necessary for the reduction of oxygen to water. The final vectorial process is the conversion of part of the redox energy of the reaction to translocate protons from inside to outside the mitochondrion. The mechanism of this reaction is not clear. Of the many suggested mechanisms [4] the most testable involve direct coupling of the translocated proton/hydroxide groups to the metal centres. Mitchell and co-workers have discussed two direct models of coupling – the O-loop [1] and the Cu_B ZOOP models [5]. We have previously provided evidence against simple O-loop models [6]. However, the Cu_B ZOOP model requires detailed information about the structure of the oxidase binuclear centre. Such information has been difficult to obtain, partly because of the problems underlying the heterogeneity of purified cytochrome

Correspondence to: J.M. Wrigglesworth, Metals in Biology and Medicine Centre, Division of Life Sciences, King's College London, Campden Hill Road, London W8 7AH, UK. Fax: +44 71 3334141.
Abbreviations: PMS, phenazine methosulfate; TMPD, *N,N,N',N'*-tetramethyl-*p*-phenylenediamine.

oxidase preparations. Recently, however, several groups have made advances in understanding the physical significance between different purification methodologies [7–9].

There are two primary forms of purified fully oxidized mitochondrial cytochrome oxidase. The fast ('pulsed') form exhibits fast internal electron transfer and cyanide binding kinetics, whilst the slow ('resting') form has much slower rates of electron transfer and cyanide binding and contains varying amounts of $g' = 12$ and $g' = 2.95$ EPR signals [10–13]. In addition to these species there are other oxidised forms of the enzyme that contain bound oxygen intermediates, the so-called 'P' and 'F' forms [7]. In terms of the parameters described above these forms behave similarly to the fast enzyme. For a more detailed description of the differences between conformational forms of the enzyme and nomenclature problems readers are referred to footnote 2 in Cooper and Salerno [13].

Low pH [8] or formate [7] convert the enzyme from the fast to the slow form whereas reduction of the Cu_B centre converts the enzyme from the slow to the fast form [6,14]. Recently, it has been possible to prepare the enzyme completely in the fast form by avoiding low pH [8,9] and/or allowing reductants to be present in the isolation procedure [7]. However, these preparations, whilst showing monophasic fast rates of internal electron transfer from haem a to haem a_3, still show biphasic formate [7] and cyanide [15] binding kinetics. In addition, haem a_3 appears to be a mixture of high and low spin [7], whereas in the slow preparations it is uniformly high spin.

The heterogeneity in these recent fast preparations led us to reconsider the homogeneity of our slow preparations, such as those prepared by the method of Kuboyama [16] or Yonetani [17]. We have taken advantage of using slow preparations that have no heterogeneity due to contamination by fast oxidase to correlate the reduction kinetics in the slow enzyme to other spectroscopic parameters (in line with a suggestion by Jones et al. [18]). We find that the rate of dithionite reduction of haem a_3 in slow enzyme is biphasic and that only the slowest rate observed ($< 0.005\ s^{-1}$) correlates with the disappearance of the $g' = 12$ signal. Optical differences are also seen between these two oxidized slow forms. Therefore both fast and slow cytochrome oxidase preparations contain two distinct conformations of the binuclear centre. The relevance of this heterogeneity for models of proton translocation mechanisms is discussed.

Materials and Methods

Slow and fast bovine heart cytochrome c oxidase was purified as previously described [7,13,16]. Stock dithionite solutions were freshly made in water, pre-bubbled with argon, and kept under argon or in sealed air-tight vessels. The solutions were not kept for longer than 15 min. The final pH of the solution following dithionite addition was either determined directly or by measuring the pH following the mixture of the same concentrations of dithionite and buffer solutions (presuming negligible enzyme buffering relative to 100 mM buffer).

The time-course of dithionite reduction of cytochrome oxidase was followed optically by use of a Cary 210 spectrophotometer (single wavelengths) or a Perkin-Elmer 356 spectrophotometer (double wavelengths). The changes in spectra with time were recorded by use of a diode array spectrometer (Hewlett Packard 8452). The deconvolution of optical changes into the % reduction of haem a and haem a_3 was calculated as described previously [6]. This presumes that the enzyme is converted from the fully oxidized to the fully reduced form following dithionite addition (reduction was finished after 30–45 min when the t_∞ point was taken). The values used for the contribution of the two haems to the absorbance changes at 444 nm and 605 nm (or 444–462, and 605–623 nm for the double wavelength experiments) varied as described in the Results section. In general, separate experiments were carried out to monitor the changes in the Soret and visible regions, although no significant differences were noted when the two were monitored simultaneously using the diode array spectrophotometer.

Unless otherwise stated all experiments were carried out at 25°C and in 100 mM Hepes, 0.5% Tween-80. The addition of dithionite to anaerobic oxidised cytochrome oxidase was carried out using a glucose/glucose oxidase/catalase system essentially as described previously [6]. To prevent peroxide formation upon addition of dithionite to oxygen [19] both the enzyme solution and the solution in which dithionite was dissolved were pre-treated with glucose oxidase and catalase.

Continuous-wave EPR measurements were recorded on a Bruker ESP300 spectrometer fitted with a TE103 rectangular cavity, a Hewlett Packard microwave frequency counter 5350B and an Oxford instruments liquid helium flow cryostat ESR900. Spectra were baseline corrected by subtraction of a cavity spectrum or water/buffer under identical conditions. In all 'kinetic' EPR experiments the EPR tubes were rapidly frozen in liquid methanol, pre-cooled in a bath of liquid nitrogen. The dithionite solution was added to the enzyme solution in a small tube and aliquots removed at the required times for freezing in EPR tubes.

All the kinetic experiments discussed in this paper were performed on the slow ('resting') form of cytochrome oxidase. It is important to remember this in the discussion of the two different rates of haem a_3 reduction by dithionite. The 'fastest' rates quoted here

are still significantly slower than those seen in fast ('pulsed') cytochrome oxidase, where even at high dithionite concentrations the rate of haem a_3 reduction is as rapid as that of haem a.

Results

Fig. 1a shows the increase in absorbance at 444 nm following the addition of 5 mM or 40 mM sodium dithionite to a slow enzyme preparation. The absorbance changes at 444 nm and 605 nm can be deconvoluted to give rates of haem a and a_3 reduction [6], presuming that haem a contributes 33% and haem a_3 67% at 444 nm, and haem a contributes 80% and haem a_3 20% at 605 nm [20]. Fig. 1b shows that haem a is reduced quickly and haem a_3 slowly (in agreement with the data of Jones et al. [18] and Wrigglesworth et al. [6]). The rate of reduction of haem a is dependent on the dithionite concentration. At the lower (5 mM) dithionite concentration there is a lag phase prior to the reduction of haem a_3, consistent with the prior need for haem a to be reduced [6,18]. The best fit to the rate of reduction of haem a_3 is a double exponential as shown by the non-random residuals for a single exponential fit (Fig. 1c). The same biphasic fit result is obtained if the deconvolution algorithm is calculated assuming [6] that the haem a and haem a_3 have identical extinction coefficients at 444 nm (results not shown). To check that this biphasicity is not an artifact of the spectral deconvolution procedure both single and double exponentials were fitted to the absorbance increase at 444 nm using only those points at least 60 s subsequent to dithionite addition, when all the haem a was reduced. Again non-random residuals were observed for the single, but not the double exponential fit. Both exponential rates are independent of enzyme concentration in the range 1–45 μM. The rate constants for a_3 reduction are given in Table I.

A number of authors have previously observed heterogeneity in the kinetics of a_3 reduction by dithionite [18], phenazine methosulphate [21], ruthenium hexammine and Cr^{2+} [22]. It is important to avoid confusion with the biphasicity reported here. The fast rate in these papers is reported as 0.1–0.4 s^{-1} and the slow rate < 0.02 s^{-1}. Thus the fast rate is probably due to contamination of these preparations with a varying proportion of fast enzyme (which show rates of a_3 reduction in excess of 0.1 s^{-1}). The slower rate discussed, but not analysed in detail, in these papers is thus seen as a composite of the two slow rates observed here. This composite slow rate is also that discussed by us previously [6,7]).

The values of the faster rate of a_3 reduction in the present experiments are highly dependent on the model used to deconvolute the haem a_3 reduction rate from that of haem a (Table I). Using a 50% contribution of

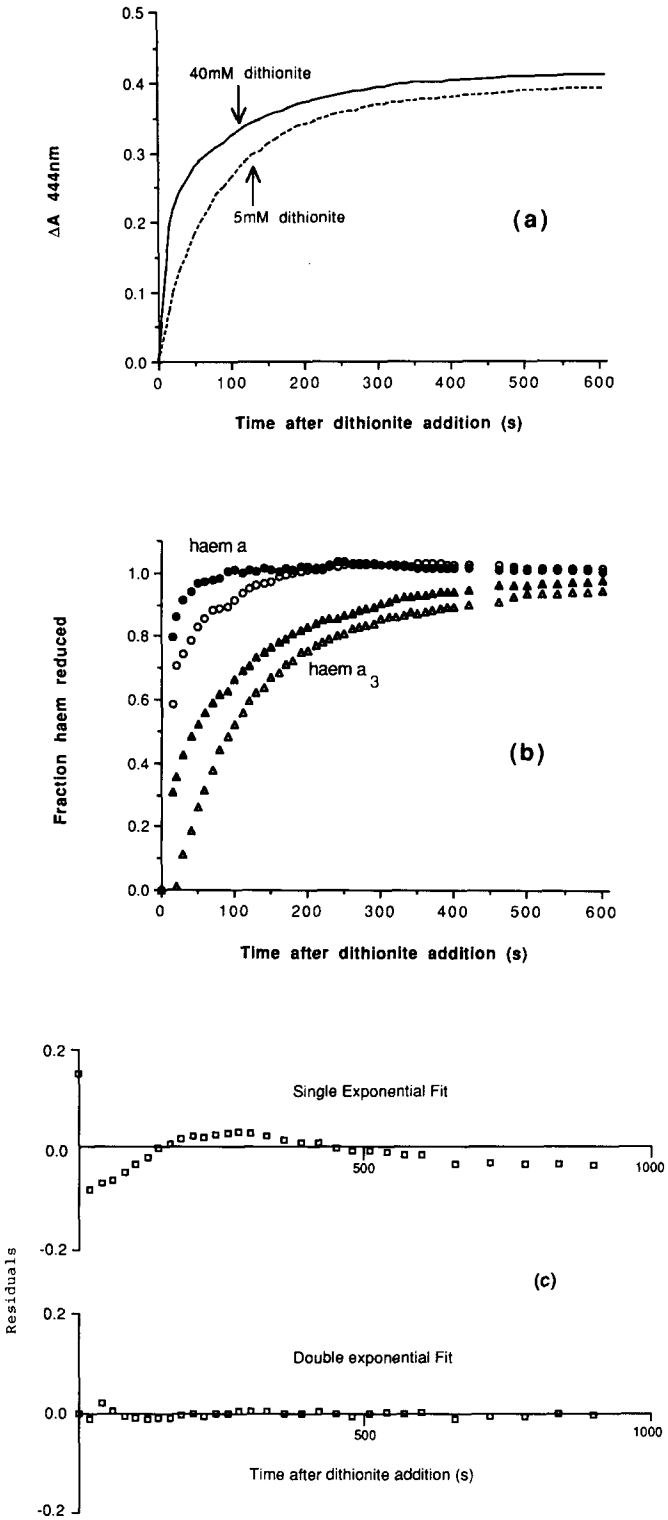

Fig. 1. Rate of reduction of slow ('resting') cytochrome oxidase by dithionite. (a) At $t = 0$ sodium dithionite (5 mM or 40 mM) was added to 2.75 μM slow cytochrome oxidase, in Hepes (100 mM) (pH 7.0), at 25°C in 0.5% Tween-80. (b) The fraction of haem a and haem a_3 reduced was calculated as stated in the text, using the absorbance changes at 444 nm and 605 nm from separate experiments. 5 mM sodium dithionite: haem a (○) haem a_3 (△); 40 mM sodium dithionite: haem a (●) haem a_3 (▲). (c) Residuals for single and double exponential fits to the deconvoluted data for haem a_3 reduction at 40 mM dithionite concentration.

TABLE I

Rate constants for dithionite reduction of haem a_3 in slow cytochrome oxidase

Conditions as for Fig. 1 (dithionite concentration = 40 mM). Data fitted to time course at 444 nm or a deconvolution algorithm with haem a_3 reduction contributing to either 50% (1/2 1/2 algorithm) or 67% (1/3 2/3 algorithm) of the absorbance increase at 444 nm. The remaining absorbance was presumed to be due to haem *a* reduction. Data were fitted to all points ($t = 0$ to $t = \infty$) or to only those points greater than 20 s subsequent to dithionite addition ($t = +20$ s to $t = \infty$). Both algorithms used a contribution of 20% for haem a_3 and 80% for haem *a* at 605 nm. Rates are quoted as means ± S.D. ($n = 3$). n.d., not determined.

Fitting procedure	Fast rate (s^{-1})	Slow rate (s^{-1})
$t = 0$ s to $t = \infty$		
ΔA444 nm time-course	n.d.	n.d.
1/3 2/3 algorithm	0.073 ± 0.0009	0.00607 ± 0.00095
1/2 1/2 algorithm	0.012 ± 0.0016	0.00403 ± 0.00026
$t = +20$ s to $t = \infty$		
ΔA444 nm time-course	0.027 ± 0.00286	0.00581 ± 0.00082
1/3 2/3 algorithm	0.022 ± 0.00324	0.00502 ± 0.00049
1/2 1/2 algorithm	0.021 ± 0.00400	0.00447 ± 0.00032

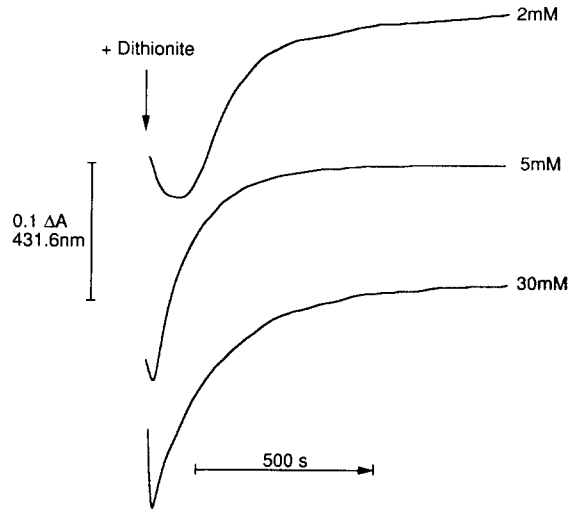

Fig. 2. Rate of carbonmonoxy-haem a_3 formation following dithionite addition to slow cytochrome oxidase in the presence of CO. Conditions as for Fig. 1 except CO was bubbled into cuvette prior to dithionite addition. The absorbance change at 431.6 nm was followed with respect to time following the addition of different concentrations of sodium dithionite as described in the figure.

haem a_3 to the absorbance at 444 nm gives a slower rate than that presuming a 33% contribution. Both rates give slower values than the (clearly) incorrect assumption that all the absorbance at 444 nm is due to haem a_3. Both models predict that at this (high) dithionite concentration all of the haem *a* is reduced after 20 s (this was confirmed by the complete removal of the g = 3.0 EPR signal of haem *a* after this time [13]). As expected, therefore, both types of deconvolution as well as the straight A444 nm time-course give similar results if only the data 20 s post dithionite addition are analysed (Table I). The values of the slower rates are less dependent on the model used because the majority of this reduction occurs after haem *a* is fully reduced.

At lower concentrations of dithionite when haem *a* is reduced more slowly a lag phase is observed before a_3 reduction reaches its maximum rate (Fig. 1). However, following the lag the same two phases of reduction occur at the same rates as seen at higher dithionite concentrations. A more direct measure of this lag phase can be seen if carbon monoxide is included in the reaction mixture at high dithionite concentrations. The absorbance at 431.6 nm (isosbestic for reduced minus oxidised high-spin haem a_3 [49]) decreases upon reduction of haem *a* but then increases upon formation of the carbonmonoxy-a_3 complex (Fig. 2). The increased lag phase in the formation of this signal at low dithionite concentrations can clearly be seen, although the final rates of carbonmonoxy-a_3 formation are independent of dithionite concentration. This lag phase is either a kinetic consequence of the dependence of the rate of reduction of haem a_3 on the concentration of reduced haem *a* or a consequence of the need for electrons to enter haem *a* prior to entering haem a_3. A similar lag phase is evident in Fig. 3 of Jones et al. [18] where the onset of photosensitivity in cytochrome oxidase is monitored at different dithionite concentrations. Analysis of the residuals again reveals that a double exponential fit is required to fit the time-course of the formation of the reduced carbonmonoxy-a_3 complex (results not shown).

The 655 nm band of cytochrome oxidase is presumed to be a marker for high spin haem a_3 [23]. Measurements of the decay of the 655 nm band also suggest that it follows a biphasic time-course with rates similar to those predicted for haem a_3 from Figures 1 (results not shown – see also Wrigglesworth et al. [6]).

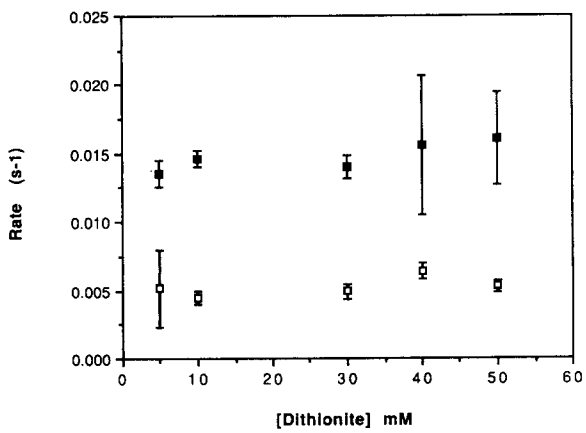

Fig. 3. Dithionite concentration dependence of the two phases of reduction of haem a_3 in slow cytochrome oxidase. Conditions as for Fig. 1. Dithionite concentration was varied and the absorbance change at 444 nm (starting at $t = +60$ s) was used for calculating the rate of the fast (■) and slow (□) phases of haem a_3 reduction.

TABLE II

Rate constants for dithionite reduction of slow cytochrome oxidase in the presence of ligands

Conditions as for Fig. 1 except that 30 mM sodium dithionite was used. Where indicated experiments were performed in the presence of 10 mM formate or CO saturated buffer. Rates were calculated from the change in absorbance at 444 nm (control, formate) or 431.6 nm (carbon monoxide), only using points greater than 60 s subsequent to dithionite addition. Rates are quoted as means ± S.D. ($n = 3$).

Ligand added	Fast rate (s^{-1})	Slow rate (s^{-1})
Control	0.020 ± 0.005	0.0051 ± 0.0016
+ Formate	0.017 ± 0.004	0.0054 ± 0.0014
+ Carbon monoxide	0.023 ± 0.006	0.0063 ± 0.0002

However, the low intensity of this absorption band makes an accurate calculation of the two rates difficult.

The values of the two rate constants for slow cytochrome oxidase reduction by dithionite are shown in Table II in the presence and absence of ligands that bind to oxidized (formate) or reduced (carbon monoxide) haem a_3. Neither ligand has a significant effect on either of the rates of a_3 reduction. The CO result is in direct contradiction to models where there is a redox, rather than a kinetic, barrier between haem a and haem a_3 [24]. It is however, consistent with the similarity between our slow rates and those seen by Jones et al. [18] in the presence of CO. The coincidence of the rates in the presence or absence of formate suggests that the reduction of haem a_3 triggers the release of formate from the enzyme. Therefore attempts to use the rate of a_3 reduction in the presence of formate to measure the off rate for formate binding may yield misleading results [25].

Redox-type models also predict that the slow rate rate of a_3 reduction is affected by dithionite concentration [24]. Fig. 3 shows that there is no effect of dithionite concentration on the rate of a_3 reduction in slow oxidase – in agreement with the findings of Jones et al. [18]. The K_m of 2 mM dithionite noted by Bickar [24] is not seen in either phase, whether using the deconvolution method or following the ΔA at 444 nm. We have previously shown, using spectral deconvolution, that varying the dithionite concentration in the range 0.9 mM to131 mM (a difference in concentration of 1.1 μM to 13.5 μM for the reactive $SO_2^{\cdot-}$ radical) has no effect on the rate of haem a_3 reduction [6]. We conclude that any effect of dithionite concentration on the rate of a_3 reduction occurs solely via the requirement that haem a has to be reduced prior to haem a_3 [6,18].

The biphasic nature of haem a_3 reduction in the slow oxidase is also apparent in the effect of pH on the rate of dithionite reduction. Lowering the pH has little effect on the faster rate, but significantly accelerates the slower rate (Fig. 4a and b). Thus the time-course of reduction becomes less biphasic as the pH is lowered. In this figure the data have been analysed using a deconvolution method from $t = 0$ (the same trends are seen if the time-courses are analysed after 20, 40 or 60

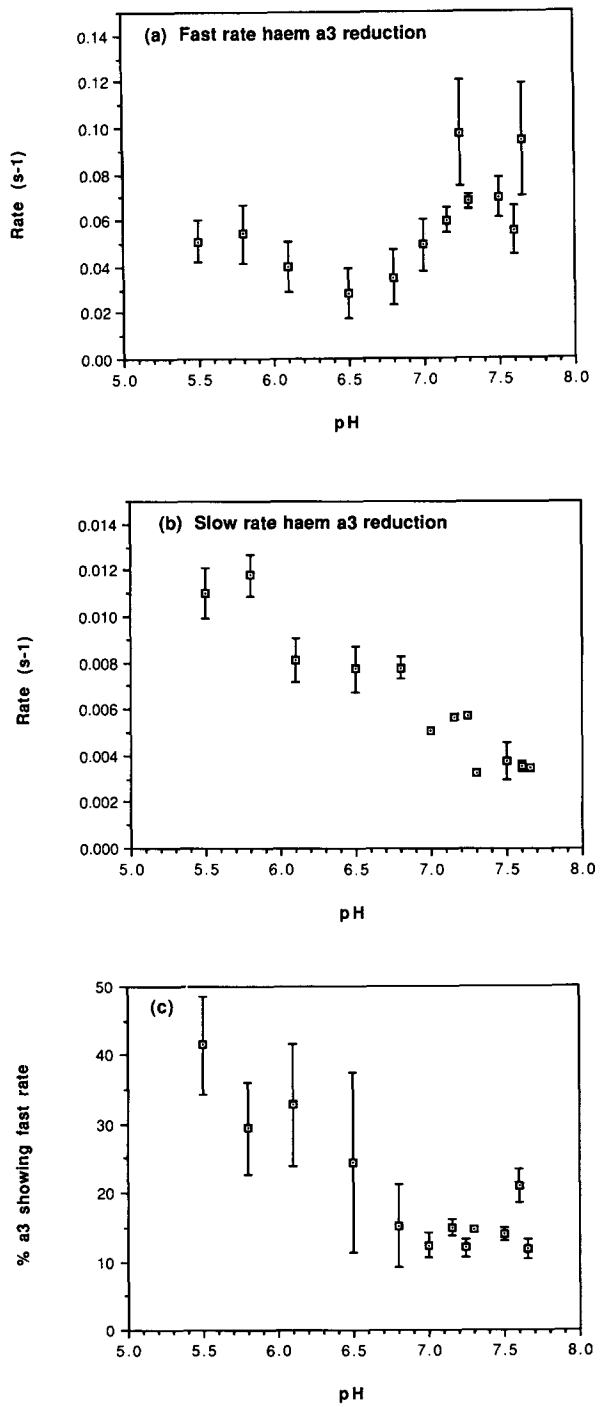

Fig. 4. Effect of pH on the two phases of reduction of haem a_3 by dithionite in slow cytochrome oxidase. Conditions as for Fig. 1 except sodium dithionite concentration used was 25 mM. The fast (a) and slow (b) rates of haem a_3 reduction were calculated using double exponential fits to the deconvoluted data. The fraction of enzyme showing the fast rate (c) was calculated from the relative amplitudes of the slow and fast fits.

s – when all the haem *a* is reduced). The use of this deconvolution method allows a comparison of the relative amplitudes of the two phases. We noted an apparent increase in the amount of the rapidly reducible form as the pH is lowered (Fig. 4c). However, it is difficult to quantify this accurately given the larger errors associated with the amplitude measurements as the pH is lowered (due to the decrease in the biphasicity of the time-course as the fast and slow rates become less distinct).

Slow forms of cytochrome oxidase contain large amounts of a $g' = 12/g' = 2.95$ EPR signal attributed to an $S = 2$ Cu_B/a_3 centre, distinct from any low spin ferric haem signal at $g' = 3.0$ [13]. The decrease in the $g' = 12$ signal following dithionite reduction correlates with that of the slower rate of haem a_3 reduction (Fig. 5). An identical time-course was obtained if the rate of decrease in the $g' = 2.95$ was followed instead, confirming the assignment of these two signals to the same form of cytochrome oxidase [13]. Given the difficulty in obtaining accurate values for the amplitudes of the two phases of a_3 reduction observed optically, it is still possible that the $g' = 12$ signal is present in both slow and fast phases if the amplitude of the fast phase observed optically is significantly lower than that of the slow phase. Then only a small fast phase of $g' = 12$ reduction would be observed and this might be lost in the errors of Fig. 5. Alternatively it is possible that the amplitude of the signal at $g' = 12$ per enzyme molecule in the faster form of a_3 is smaller than that present in the slower form. Again this would result in only a small change in signal intensity during the fast phase of a_3 reduction. However, under the conditions used here

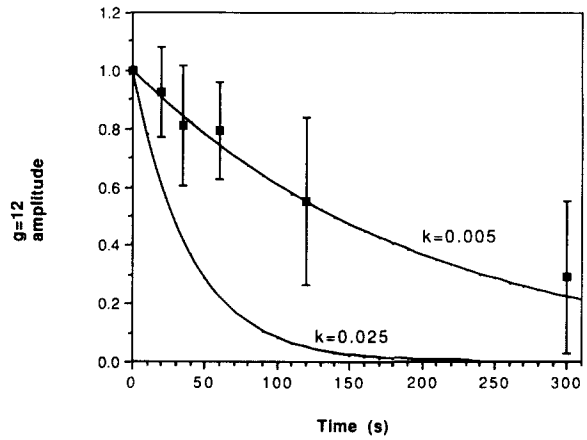

Fig. 5. Rate of disappearance of $g' = 12$ EPR signal following dithionite addition to slow cytochrome oxidase. Conditions as for Fig. 1 except enzyme concentration was 30 μM. Samples were frozen and the EPR spectra obtained as described in Materials and Methods. Points are the peak minus trough of the $g' = 12$ EPR signal (means $\pm$ S.D., $n = 3$). The lines on the graph represent the fast ($k = 0.025$) and slow ($k = 0.005$) rates of haem a_3 reduction observed optically. EPR conditions as for Fig. 6.

we could detect no major difference in the shape of the $g' = 12$ signal during the time course of reduction (although some small differences between the spectra of the fully oxidised enzyme and the half-reduced enzyme were noted by Hagen [26]).

The most likely explanation of the data in Fig. 5, however, is that only the fraction of the enzyme that is reduced slowly contributes to the $g' = 12$ EPR signal. If this is the case one would expect the rate of disappearance of the $g' = 12$ EPR signal to follow the pH dependence of the slow phase rather than the fast

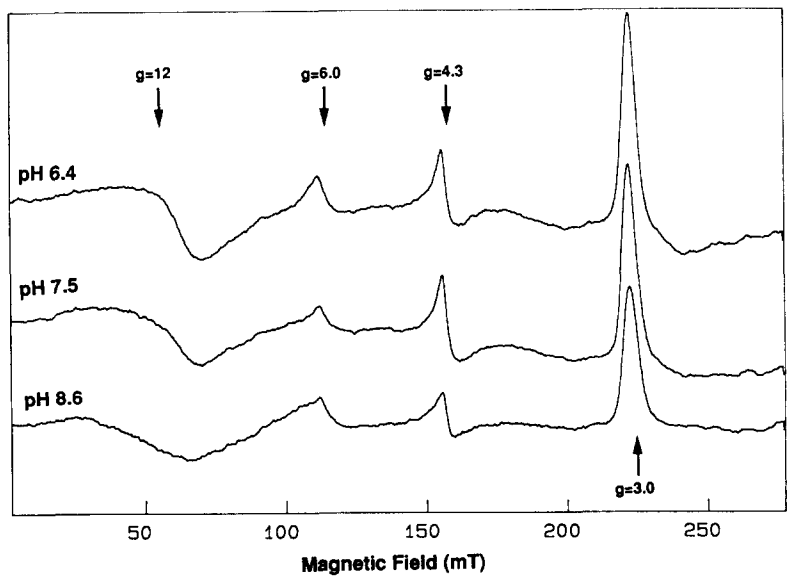

Fig. 6. pH dependence of the intensity and lineshape of the cytochrome oxidase $g' = 12/g' = 2.95$ EPR signals. EPR spectra of cytochrome oxidase samples (30 μM) frozen 30 min after incubation at the indicated pH. EPR conditions: temperature, 10 K; microwave frequency, 9.36 GHz; modulation frequency, 100 kHz; modulation amplitude, 10 G; receiver gain, $1.6 \cdot 10^5$; time-constant, 0.33 s; sweep time, 33 G s^{-1}; signal is average of two scans.

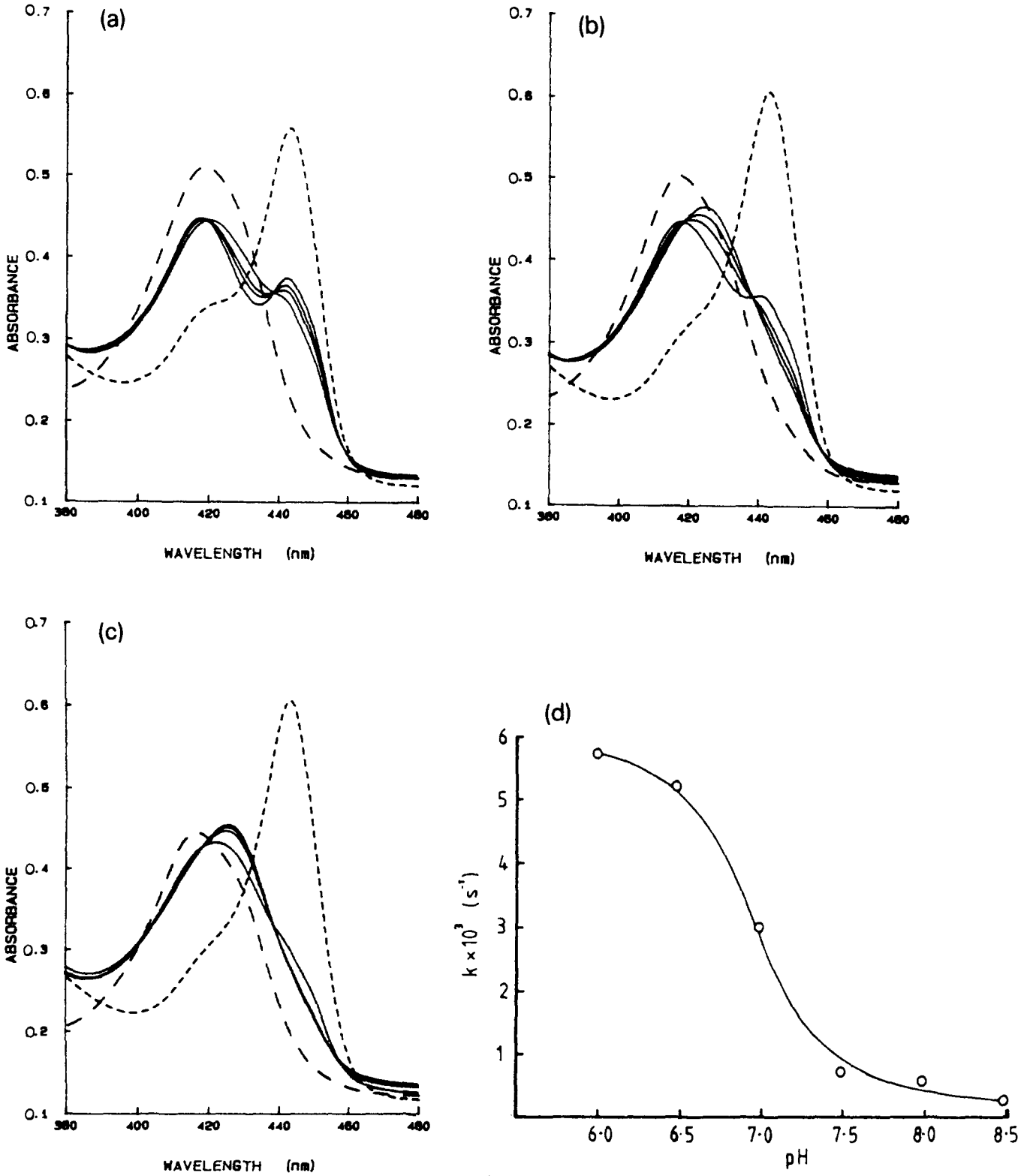

Fig. 7. pH dependence of the rate of the spin-state change in haem a_3 following aerobic addition of ascorbate/TMPD to slow cytochrome oxidase. Turnover was initiated by the addition of ascorbate (15 mM) plus TMPD (0.25 mM) to a sample of slow cytochrome oxidase (3.56 μM) in potassium phosphate buffer (100 mM) at (a) pH 8.5, (b) pH 7.5, and (c) pH 6.5. Repetitive scans were taken (scan time 50 s) immediately following substrate addition and then after 2 min, 4 min and 10 min (solid lines). A final reduced spectrum was taken after 15 min (dotted line). The spectral scans taken during turnover show decreasing absorption at 444 nm with time and a shift to the red in the absorbance maxima around 420 nm. (d) pH dependence of the apparent (slow) rate constant for haem a_3 spin state change (monitored at 433 nm minus 413 nm).

phase, i.e., disappear more slowly at high pH. This was tested by determining the amount of $g' = 12$ remaining 2 min after dithionite addition as a function of pH. Over the pH range 5.5–8.0 it was found that the amount of $g' = 12$ signal remaining was consistent with that calculated from the pH dependence of the slow rate alone. The presence of formate had no significant effect on these results.

It is therefore clear that only the slow phase of a_3 reduction is associated with the $g' = 12/g' = 2.95$ EPR signals. Either there are two forms of the slow enzyme with different rates of reduction, or the $g' = 12$ form is not reducible by dithionite and the slow reduction rate is therefore a function of the conversion of the $g' = 12$ form into the EPR-silent form. If the latter was true one might expect the equilibrium of the two forms to be affected by pH, given the effect of pH on the slow rate constant for dithionite reduction. Specifically one would expect more of the $g' = 12$ form at high pH. We therefore studied the effect of pH on the $g' = 12$ signal in slow cytochrome oxidase (Fig. 6). There appears to be no significant increase in the amount of $g' = 12/g' = 2.95$ signal at high pH, suggesting that the two forms of slow enzyme are both reducible by dithionite and that the slower rate observed is a direct measure of the reduction of the binuclear centre exhibiting the $g' = 12/g' = 2.95$ signal. However, one must be cautious about this conclusion as there is clearly a broadening of both the $g' = 12$ and $g' = 2.95$ signals at higher pH's. Given the difficulty of quantifying even spin EPR signals [26,27] one must be very wary of comparing intensities of such EPR signals, especially when the lineshape is not identical. Suffice to say that a 30 minute incubation at increasing pH yields no significant increase in either the peak to trough at $g' = 12$, nor a truncated integral between zero field and 950 G. This conclusion is similar to that reached by Baker et al. [8] upon raising the pH of a slow preparation from pH 6.8–8.6, although they do not mention the EPR line broadening phenomenon.

The line broadening associated with both the $g' = 12$ and $g' = 2.95$ signals at higher pH is also significant for two other reasons. First it again shows the connection between the two signals [13]. It also means that one must be careful in excluding the presence of small amounts of $g' = 12$ in essentially fast oxidase preparations; in order to keep these preparations fast they are maintained at pH 8.5, under which conditions it is more difficult to detect the $g' = 12$ signal.

The very slow reduction rate observed here is present when other reductants are used besides dithionite to reduce slow cytochrome oxidase anaerobically (e.g., PMS [21]). However, the same process also occurs aerobically (Fig. 7). This can be seen in the spin state changes involved following the aerobic addition of ascorbate/TMPD to slow cytochrome oxidase [6]. Under these (turnover) conditions the haem a_3 remains fully oxidised due to the kinetics of the oxygen reaction. The absorbance at 444 nm is therefore due to reduced haem a. Initially the haem a becomes rapidly reduced (as in the anaerobic experiments following dithionite addition) and there is an increase in absorbance at 444 nm. However, as the binuclear centre is reduced the haem a reduction level drops as the enzyme converts to the active (fast) form and the internal electron transfer rate rises. Therefore the drop in the 444 nm peak with time is equivalent to the rate of a_3 reduction in the slow enzyme. There are also changes in the oxidised a_3 spectra with time. The shift to the red in the absorbance spectra (419 nm to 428 nm) is consistent with the slow ('resting') to fast ('pulsed') transition and is also a measure of the rate of reduction of haem a_3 in the slow enzyme [6,7]. The rate of the a_3 spin state change and the decrease in haem a reduction are both slowed by an increase in pH (Fig. 7a–c). The slow rate of spin state change can be followed as a function of time by using the wavelength pair 433–413 nm [6]. The pH effect on the reduction rate is the same as that observed in the dithionite reduction of slow cytochrome oxidase, confirming that the same process is being observed.

The two phases of dithionite reduction reveal that the slow enzyme has two different spectroscopic forms – one with the $g' = 12$ signal and one that is EPR silent. We therefore decided to re-analyse the spectral changes occurring during the two phases of reduction in order to determine whether there were corresponding differences in the optical spectra. In order to detect the two forms independently a diode-array spectrometer was used and the experiment performed at high pH to ensure good separation of the two phases (Fig. 8). After 12 s full reduction of haem a and Cu_A had occurred as shown by the changes at 605 nm and 830 nm. Therefore the spectral changes observed after 12 s should be only due to haem a_3 reduction. It can be seen from Fig. 8a that there is no isosbestic point for the reduction of haem a_3. Presuming that the reduced haem a_3 spectrum is independent of enzyme heterogeneity we take this to indicate that there are different optical spectra corresponding to the two forms of oxidised slow enzyme. This can be seen more clearly by reduced minus oxidised difference spectra (Fig. 8b) taken at different times after dithionite reduction. The difference spectra taken at later times (i) is blue-shifted relative to that taken at earlier times (ii). An oxidised minus oxidised spectrum for the two forms of the enzyme can then be computed by subtracting the two difference spectra (again presuming that the reduced enzyme is optically homogeneous). This double difference spectra now represents the oxidised spectra of the EPR-silent form minus the oxidised spectra of the $g' = 12$ species. It shows clearly a peak at 433 nm and a

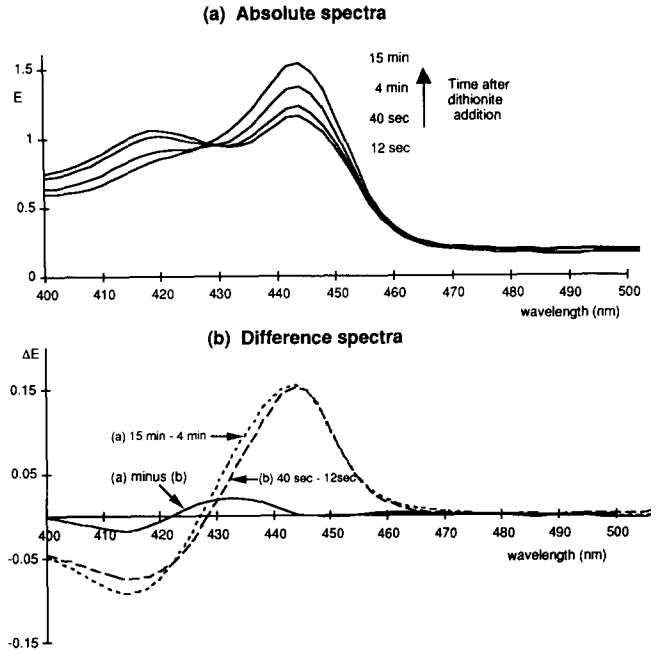

Fig. 8. Optical spectra of haem a_3 at different times following dithionite addition to slow cytochrome oxidase. Diode array spectra of cytochrome oxidase taken at different times subsequent to dithionite addition (a). The spectra were subtracted one from another to determine whether the spectrum of haem a_3 being reduced was different for the fast and slow rates (b). For comparison purposes the late and early difference spectra were normalised to be identical at 444 nm. The double difference spectra was then calculated: (15 min–4 min) – (40 s–12 s).

trough at 413 nm. Therefore the slowly reducible form (containing the $g' = 12$ and $g' = 2.95$ EPR signals) has a blue-shifted Soret peak relative to the EPR-silent form.

These difference spectra are reminiscent of those seen in the Soret region upon the formation of the 580 or 607 nm complexes of cytochrome oxidase (the so-called F and P forms, one of which is associated with the formation of a ferryl Fe(IV) = O species). It is possible for dithionite to produce H_2O_2 upon reaction with oxygen and H_2O_2 reaction with the oxidase generates these F and P forms. However, the experiments of Fig. 8 were carried out in the presence of catalase and all samples were made anaerobic prior to dithionite addition by treatment with glucose and glucose oxidase. Furthermore, no spectral differences were seen at 580 and 607 nm (or elsewhere in the visible region) between the slow and fast phases of dithionite reduction. Therefore we feel confident in correlating the increased amount of the 413 nm transition with the $g' = 12/g' = 2.95$ EPR signal.

Discussion

Time-course of haem a_3 reduction

These results clearly show that there is heterogeneity in the reduction of slow ('resting') cytochrome oxidase by dithionite. We have shown that the kinetic differences are mirrored in spectroscopic differences in both haem a_3 (optical spectra) and the nature of the coupling between haem a_3 and Cu_B (EPR spectra). This heterogeneity explains the difficulties associated with simple deconvolution algorithms (Table I) even in the slow ('resting') enzyme where there is a large difference in the rate of reduction of haem a and haem a_3. The use of such algorithms to determine the % of haem a_3 reduced in the aerobic steady state [28] is therefore likely to yield misleading results (especially when there is likely to be 'P' and 'F' forms present in addition to ferric a_3).

Our results show that both populations of enzyme in the slow ('resting') preparation represent a significant % of enzyme molecules; the exact percentage is difficult to calculate because of the errors associated with the amplitude measurements (Fig. 4) and the problems with the deconvolution method (it also depends on knowing the extinction coefficients for the two forms of the slow enzyme). By direct quantitation of the $g' = 12$ EPR signal [26] it has been suggested that the $g' = 12$ signal comes from 100% of enzyme molecules. There are several assumptions made in the quantitation of integer spin EPR signals and our results show this value is likely to be an overestimation. However, in our Kuboyama slow preparation the % of $g' = 12$ enzyme does not appear to be as low as the 20% suggested by Hill et al. [29].

What determines the rate of haem a_3 reduction in the slow enzyme?

The fact that changing the dithionite, CO and O_2 concentration has no affect on the rate of a_3 reduction is contrary to the model proposed by Bickar et al. [24] where the redox potential of haem a_3 in slow ('resting') cytochrome oxidase is significantly below that of haem a_3 in fast ('pulsed') cytochrome oxidase. If the equilibrium model is not correct, then the electron transfer rate must be slower between haem a and the binuclear centre in the slow enzyme. We favour a model where the ligand structure of the active site is different in the slow and fast enzymes [7]; this affects the kinetics of a_3 reduction due to the re-organisation energy involved in the displacement of the bridging ligand. We have previously shown that the limiting factor in the reduction of slow oxidase is the addition of a single electron to form the species a_3^{3+}/Cu_B^+ [6]. Once the enzyme is in the form a_3^{3+}/Cu_B^+ the bridging ligand is broken and the second electron enters quickly. This is the reason why insignificant amounts of high spin haem a_3 are detectable by EPR during the time-course of a_3 reduction [13,30].

The rate in the slow enzyme can be accelerated by the addition of cytochrome c [24,25]. It is possible that global conformational changes in the slow enzyme are

the cause of this increase; however, this appears unlikely given that the increased rate only occurs when there is a redox-active metal in the cytochrome *c* active site [24]. Furthermore, any conformational change could not be equivalent to the slow-fast transition as we find that oxidised cytochrome *c* does not affect the EPR spectrum of the slow enzyme (results not shown). Furthermore, the cytochrome *c*-enhanced rate of a_3 reduction is still significantly slower than the rate in the fast enzyme; the latter is limited by the rate of haem *a* reduction even at high dithionite concentrations (results not shown). Our current explanation for this cytochrome *c* effect is that there is some direct reduction of the binuclear centre by cytochrome *c*, bypassing haem *a*, though possibly not Cu_A.

Ligands of the binuclear centre in the slow enzyme

Our knowledge of the structure of the binuclear centre in the slow enzyme is still incomplete (as is the case with the fast enzyme). However, recent data have shed some interesting new light on the problem, especially the role of formate. Formate has been shown to induce the fast-slow transition by several methods. The binuclear centre in the intrinsic slow (low pH-induced) and formate-induced slow enzyme share the following properties:

(i) A $g' = 12$ EPR signal with similar lineshape, temperature and microwave power saturation properties [13].

(ii) A $g' = 2.95$ EPR signal with similar lineshape, temperature and microwave power saturation properties [31].

(iii) Similar optical spectra [7].

(iv) Similar Raman spectra [32,33].

(v) A spin state of $S = 2$ (via magnetic susceptibility [19]).

(vi) Similar cyanide binding kinetics [7,34].

(vii) Similar biphasic reduction kinetics with dithionite – with similar pH dependence (this paper).

(viii) Similar enhancement of the reduction rate by cytochrome *c* [24,25].

No other ligand shares these properties with the intrinsic-resting ligand. The conclusion is either that the intrinsic ligand in the resting enzyme is similar to formate, or that formate does not bind at the binuclear centre, but induces a conformational change in the enzyme that causes the fast-slow transition [19]. We favour the former hypothesis and suggest that the conserved carboxylate residue (Glu-286) is a likely candidate. Fig. 9 shows that current molecular models of cytochrome oxidase can be constructed consistent with this residue bridging in the active site. However, such models require that his284 on helix VI be distal rather than proximal to haem a_3, in contrast to the model of Shapleigh et al. [35]. There is little evidence to help choose which helix, VI or X, provides the proximal

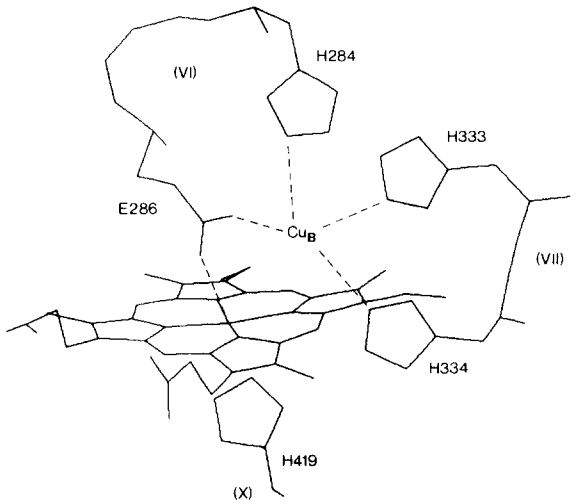

Fig. 9. A model of slow cytochrome oxidase. Possible arrangement of coordinating ligands in the binuclear centre of cytochrome oxidase. Cu_B coordinates to the two histidines of helix VII plus one histidine of helix VI, leaving the conserved glutamic acid residue (E286) to bridge between Cu_B and the iron of haem a_3 (for clarity, isoprenoid side chain of haem a_3 is omitted).

histidine to haem a_3. Placing helix VI distal to haem a_3 would allow his284 to act as one of the three histidines coordinating to Cu_B and provide the conserved glu286 as a flexible bridging ligand between Cu_B and the iron of haem a_3 (Fig. 9).

The spectral properties of the bromide complex of oxidase may also be explained by the fact that bromide can bridge over the same distance as formate – five coordinate CuII-CuII dimers can be made that are bridged by formate, bromide and phenolate simultaneously [36]. Whilst we favour a carboxylate bridging ligand to induce the $g' = 12$ EPR signal, it is possible that the carboxylate binds to Cu_B alone and perturbs the Fe-Cu coupling sufficiently to have the same effect [34].

pH and heterogeneity in the binuclear centre: relevance to the mechanism of proton translocation

If the presence of a bridging carboxylate ligand is the difference between the fast and slow forms of the enzyme, what is the reason for the heterogeneity in the slow forms observed in this paper (both in reduction kinetics and optical/EPR spectroscopy)? We favour a model where Cu_B is penta-coordinate in the slow enzyme with three histidines, the bridging carboxylate ligand and a fifth ligand that is water or hydroxide. It is well established that it is possible to bind two ligands to the binuclear centre [29,37,38]. One free position is clearly that of the sixth position to haem a_3. However, there is good evidence for a free ligand position on Cu_B that can bind exogneous ligands: e.g., Br^- [7], Cl^- [7], NO [37], SH^- [29] CO [39] and CN^- [40]. Furthermore, the similar increase in the rate of binding of

many of these ligands at low pH [7] suggests that OH^- [41, 42] may be present at this site in the isolated enzyme. Direct evidence for a nearby OH^- or H_2O comes from ENDOR of the Cu_B EPR signal [43].

In agreement with Mitchell's mechanism for Cu involvement in proton translocation [5] we suggest that the free Cu_B ligand is $OH^-$when Cu_B is cupric and H_2O when Cu_B is cuprous. Presuming that the two forms of the slow enzyme have the same oxidation state this would yield the two structures shown below:

Fast reduction, EPR silent Slow reduction, $g = 12/g = 2.95$ EPR

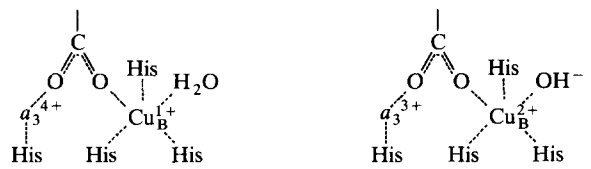

We favour this model over one where Fe^{IV} is EPR detectable for several reasons:

(i) The (presumed) higher redox potential of Fe^{IV} should result in a faster reduction rate from haem *a*.

(ii) The hydroxide ligand on Cu^{II} could be responsible for both the pH dependence of the $g' = 12/g' = 2.95$ lineshape and the pH dependence of the slow rate of dithionite reduction.

(iii) The optical spectrum of the EPR-silent form shows a similar red-shift in the Soret spectrum to that seen in the $Fe^{IV} = O$ complex of the enzyme.

In this model Fe^{IV} is EPR silent and could therefore be low spin ($S = 1$) or high spin ($S = 2$). The slower rate of a_3 reduction could be due either to a slower rate of reduction of the ferric form or could represent the rate of conversion of the ferric species to the more rapidly reducible ferryl state.

A similar model can be used to explain the heterogeneity in the fast enzyme as well. In this case we would expect Cu_B to be four coordinate (three histidines and a hydroxide/water). There also exists the possibility that haem a_3 itself coordinates to a hydroxide molecule [41,44–47]. This would explain the presence of both high and low spin haem a_3 in fast oxidase preparations [7]. Mossbauer data of the oxidized *Thermus thermophilius* enzyme also suggest that the haem a_3 spin state is heterogeneous with $S = 0$ and $S = 2$ components [48].

There are now good spectroscopic data suggesting hydroxide ligation to Cu_B in both the fast and slow enzyme molecules, as well as the presence of a nearby conserved carboxylate residue. Cu_B has also been shown to have a flexible ligation state. Combined with the recent evidence that proton translocation appears to be involved with changes in the binuclear centre [41] we feel that there is growing evidence for the involvement of Cu_B/hydroxide translocation mechanisms, as originally proposed by Mitchell [5].

Acknowledgements

C.E.C. is grateful for a King's College Research Fellowship and a Medical Research Council Training Fellowship. S.J. is in recept of a studentship from SERC. We would like to thank Jim Heal and Brian Bainbridge (KCL) for the use of the diode array spectrometer and Richard Cammack, Andy White and Ruth Williams (KCL) for assistance with EPR spectroscopy.

Note added in proof (received 12 May 1993)

Since the submission of this paper a model with similar characteristics to that shown in Fig. 9 has been proposed by Brown, S., Moody, A.J., Mitchell, R. and Rich, P.R. (1993) FEBS Lett. 316, 216–223.

References

1 Mitchell, P., Mitchell, R., Moody, A.J., West, I.C., Baum, H. and Wrigglesworth, J.M. (1985) FEBS Lett. 188, 1–7.
2 Rich, P.R., West, I.C. and Mitchell, P. (1988) FEBS Lett. 233, 25–30.
3 Wikström, M. (1984) Nature 308, 558–559.
4 Wilson, M.T. and Bickar, D. (1991) J. Bioenerg. Biomemb. 23, 755–771.
5 Mitchell, P. (1987) FEBS Lett. 222, 235–245.
6 Wrigglesworth, J.M., Elsden, J., Chapman, A., Van der Water, N. and Grahn, M.F. (1988) Biochim. Biophys. Acta 936, 452–464.
7 Moody, A.J., Cooper, C.E. and Rich, P.R. (1991) Biochim. Biophys. Acta 1059, 189–207.
8 Baker, G.M., Noguchi, M. and Palmer, G. (1987) J. Biol. Chem. 262, 595–604..
9 Brandt, U., Schägger, H. and Von Jagow, G. (1989) Eur. J. Biochem. 182, 705–711.
10 Greenaway, F.T., Chan, S.H.P. and Vincow, G. (1977) Biochim. Biophys. Acta 490, 62–78.
11 Beinert, H. and Shaw, R.W. (1977) Biochim. Biophys. Acta 462, 121–130.
12 Brudvig, G.W., Stevens, T.H., Morse, R.H. and Chan, S.I. (1981) Biochemistry 20, 3912–3921.
13 Cooper, C.E. and Salerno, J.C. (1992) J. Biol. Chem. 267, 280–285.
14 Brunori, M., Colosimo, A., Rainoni, G., Wilson, M.T. and Antonini, E. (1979) J. Biol. Chem. 254, 10769–10775.
15 Moody, A.J. and Rich, P.R. (1991) Biochem. Soc. Trans. 19, 262.
16 Kuboyama, M., Yong, F.C. and King, T.E. (1972) J. Biol. Chem. 247, 6375–6383.
17 Yonetani, T. (1960) J. Biol. Chem. 235, 845–852.
18 Jones, G.D., Jones, M.G., Wilson, M.T., Brunori, M., Colosimo, A. and Sarti, P. (1983) Biochem J. 209, 175–182.
19 Barnes, Z.K., Babcock, G.T. and Dye, J.L. (1991) Biochemistry 30, 7597–7603.
20 Antalis, T. and Palmer, G. (1982) J. Biol. Chem. 257, 6194–6206.
21 Halaka, F.G., Babcock, G.T. and Dye, J.L. (1981) J. Biol. Chem. 256, 1084–1087.
22 Greenwood, C., Brittain, T., Brunori, M. and Wilson, M.T. (1977) Biochem. J. 165, 413–416.
23 Beinert, H., Hansen, R.E. and Hartzell, C.R. (1976) Biochim. Biophys. Acta 423, 339–355.
24 Bickar, D., Turrens, J.F. and Lehninger, A.L. (1986) J. Biol. Chem. 261, 14461–14466.
25 Nicholls, P. (1976) Biochim. Biphys. Acta 430, 13–29.
26 Hagen, W.R. (1982) Biochim. Biophys. Acta 708, 82–98.

27 Hendrich, M.P. and Debrunner, P.G. (1989) Biophys. J. 56, 489–506.
28 Capitanio, N., de Nitto, E., Villani, G., Capitanio, G. and Papa, S. (1990) Biochemistry 29, 2939–2945.
29 Hill, B.C., Woon, T.-C., Nicholls, P., Peterson, J., Greenwood, C. and Thomson, A.J. (1984) Biochem. J. 224, 591–600.
30 Hartzell, C.R., Hansen, R.E. and Beinert, H. (1973) Proc. Natl. Acad. Sci. USA 70, 2477–2481.
31 Cooper, C.E., Moody, A.J., Rich, P.R., Wrigglesworth, J.M. and Ioannidis, N. (1991) Biochem. Soc. Trans. 19, 259S.
32 Woodruff, W.H., Dallinger, R.F., Antalis, T.M. and Palmer, G. (1981) Biochemistry 20, 1332–1338.
33 Babcock, G.T. (1988) in Biological Applications of Raman Spectroscopy (Spiro, T.G., eds.), pp. 294–346, Wiley, New York.
34 Schoonover, J.R. and Palmer, G. (1991) Biochemistry 30, 7541–7550.
35 Shapleigh, J.P., Holster, J.P., Tecklenburg, M.M.J., Kim, Y., Babcock, G.T., Gennis, R.B. and Ferguson-Miller, S. (1992) Proc. Natl. Acad. Sci. USA 89, 4786–4790.
36 Adams, H., Candeland, G., Crane, J.D., Fenton, D.E. and Smith, A.J. (1990) J. Chem. Soc. Chem. Commun. 93–95.
37 Stevens, T.H., Brudvig, G.W., Bocian, D.F. and Chan, S.I. (1979) Proc. Natl. Acad. Sci. USA 76, 3320–3324.
38 Hill, B.C., Brittain, T., Eglinton, D.G., Gadsby, P.M.A., Greenwood, C., Nicholls, P., Peterson, J., Thomson, A.J. and Woon, T.C. (1983) Biochem. J. 215, 57–66.
39 Woodruff, W.H., Einarsdóttir, O., Dyer, R.B., Bagley, K.A., Palmer, G., Atherton, S.J., Goldbeck, R.A., Dawes, T.D. and Kliger, D.S. (1991) Proc. Natl. Acad. Sci. USA 88, 2588–2592.
40 Yoshikawa, S. and Caughey, W.S. (1990) J. Biol. Chem. 265, 7945–7958.
41 Mitchell, R., Mitchell, P. and Rich, P.R. (1992) Biochim. Biophys. Acta 1101, 188–191.
42 Reed, C.A. and Landrum, J.T. (1979) FEBS Lett. 106, 265–267.
43 Cline, J., Reinhammer, B., Jensen, P., Venters, R. and Hoffman, B.M. (1983) J. Biol. Chem. 258, 5124–5128.
44 Karlsson, B. and Andréasson, L.E. (1981) Biochim. Biophys. Acta 635, 73–80.
45 Lanne, B., Malmström, B.G. and Vänngård, T. (1979) Biochim. Biophys. Acta 545, 205–214.
46 Han, S. and Ching, Y.-C. (1989) J. Biol. Chem. 264, 6604–6607.
47 Papadopoulos, P.G., Walter, S.A., Li, J. and Baker, G.M. (1991) Biochemistry 30, 840–850.
48 Kent, T.A., Münck, E., Dunham, W.R., Filter, W.F., Findling, K.L., Yoshida, T. and Fee, J.A. (1982) J. Biol. Chem. 257, 12489–12492.
49 Nicholls, P. and Hildebrandt, V. (1978) Biochem. J. 173, 65–72.